AN EFFICIENT AND EFFECTIVE COLOR FILTER ARRAY DEMOSAICKING METHOD

Nai-Xiang Lian and Yap-Peng Tan

School of Electrical and Electronic Engineering
Nanyang Technological University, Singapore

ABSTRACT

To reduce the cost and size, most digital still cameras (DSCs) capture only one color value at each pixel, and the results — color filter array samples — are then interpolated by a demosaicking method to construct a full-color image. Many advanced demosaicking methods have been proposed recently. However, the high complexity of these methods could prevent them from being used in DSCs. In this paper we propose an efficient and effective demosaicking method, which substitutes high-frequency component of color values in the spatial rather than frequency domain. We also propose a simple ternary, anisotropic interpolation scheme to obtain an initial full-color image required in the spatial-domain high-frequency substitution. Experimental results show that the proposed method can outperform recent state-of-the-art methods in terms of both PSNR performance and perceptual results, at the same time reducing the computational cost substantially.

Index Terms – Color filter array, Demosaicking, Low-pass filter, Interpolation,

1. INTRODUCTION

To reduce the cost and size, most digital still cameras (DSCs) use one single sensor overlaid with a color filter array (CFA) to capture one of the three color values (red, green, blue) at each pixel. Figure 1 shows the most popular Bayer CFA pattern [1]. The two missing color values of each pixel are then interpolated to construct a full-color image, a process that is known as CFA demosaicking.

Existing work has shown that substantial correlation among neighboring pixels allows CFA samples to be demosaicked into a full-color image using such simple methods as bilinear and bicubic interpolations. However, these isotropic interpolation methods often oversmooth edges. An image of better quality can be obtained by using pixel values along a locally smooth direction, or in other words, by using a scheme that is anisotropic according to edge direction. The edge indicator can be computed directly from CFA samples [2] or based on some energy criteria [3]. Although advanced anisotropic methods may further improve the demosaicking performance, they also increase the computational cost [3].

The other useful property for demosaicking is inter-color correlation. Since color-difference images are generally smooth and more suitable for interpolation [4], applying interpolation in these images can lead to better demosaicking performance [5, 6, 3]. In particular, Gunturk *et al.* found that the high-frequency contents among color planes are strongly correlated, with near-to-1 correlations [7]. Based on this property, they proposed using the high-frequency wavelet coefficients of green plane, which is more densely sampled in a Bayer CFA, to construct the less densely sampled red and blue planes [7]. Their method achieves good performance and becomes a popular benchmark algorithm in CFA demosaicking literature.

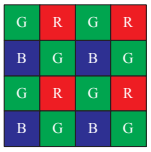

Fig. 1. Bayer color filter array

However, exploiting inter-color correlation requires as reference a color plane of full resolution, which is unavailable from CFA samples and needs to be estimated. The estimation error of the reference plane affects subsequent demosaicking operations—interpolation of color differences [4] or high-frequency substitution [7]. To minimize the impact, some existing work used a large filter to obtain a more accurate reference plane, such as a filter size of 11×11 in [5] and 21×21 in [3]. Some other work iterated the operations (e.g., Li [6] repeated the interpolation in color-difference images and Gunturk *et al.* iterated the high-frequency substitution [7]). All these methods inevitably increase the demosaicking complexity, which could prevent the methods from being used in DSCs due to limited computational resources.

In this paper we propose an efficient and effective method which comprises a spatial-domain substitution scheme for estimating the high-frequency information of missing color values (Section 2) and a ternary anisotropic interpolation scheme for estimating an initial full-color image required in the substitution (Section 3). Experimental results in Section 4 show that our proposed method outperforms four recent state-of-the-art methods in both PSNR performance and perceptual results, while having a much lower computational complexity.

2. SPATIAL DOMAIN HIGH-FREQUENCY SUBSTITUTION

We first review the method proposed by Gunturk *et al.* [7] for substituting high-frequency information in wavelet domain. Their method exploits the similarity of high-frequency components across three color planes. Let h_i, $i = 0, 1$, be the analysis wavelet filters. By wavelet transform, the filters separate an initial full-color plane $\bar{\mathcal{C}} \in \{\bar{R}, \bar{G}, \bar{B}\}$ into dissimilar low-frequency and similar high-frequency components,

$$\begin{aligned} \bar{\mathcal{C}}_{w_l} &= \bar{\mathcal{C}} * h_0 \\ \bar{\mathcal{C}}_{w_h} &= \bar{\mathcal{C}} * h_1 \end{aligned} \tag{1}$$

where $*$ denotes the convolution operator. As the green plane is more densely represented in Bayer CFA samples, and hence its

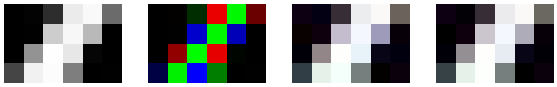

(a) (b) (c) (d)

Fig. 2. (a) Original image, (b) CFA samples, and the results of performing high-frequency substitution in (c) wavelet domain, and (d) spatial domain

Fig. 3. Test images (referred to as Image 1 to Image 10).

high-frequency information is better preserved, Gunturk's method uses the high-frequency component $\mathcal{F}_{w_h}$ from an estimated full-resolution green plane $\mathcal{F}$ to substitute the high-frequency component, $\bar{\mathcal{C}}_{w_h}$, of the red and blue planes as follows:

$$\mathcal{C} = \bar{\mathcal{C}}_{w_l} * g_0 + \mathcal{F}_{w_h} * g_1 \tag{2}$$

where g_i, $i = 0, 1$, are the synthesis wavelet filters.

However, such substitution incurs high computational complexly. Even for the simple 5-3 wavelet used in [7], the wavelet transform and its inverse processes require $32MN$ multiplications and $32MN$ additions. Iterating the substitution for better results leads to $384MN$ multiplications and $384MN$ additions.

To avoid the complex wavelet transform, we propose to perform the high-frequency substitution in spatial domain. Specifically, we use a low-pass filter f_l to separate the low and high-frequency components as follows:

$$\begin{aligned} \bar{\mathcal{C}}_{s_l} &= \bar{\mathcal{C}} * f_l \\ \bar{\mathcal{C}}_{s_h} &= \bar{\mathcal{C}} - \bar{\mathcal{C}}_{s_l} \end{aligned} \tag{3}$$

and then substitute the reference high-frequency component $\mathcal{F}_{s_h}$ for that of the other two color planes, as follows:

$$\mathcal{C} = \bar{\mathcal{C}}_{s_l} + \mathcal{F}_{s_h} \tag{4}$$

The following lemma shows that the substitution in the spatial domain (4) and that in the wavelet domain (2) lead to the same result.

Lemma 1 *Using the low-pass filter $f_l = h_0 * g_0$, performing substitution of high-frequency information in the spatial domain (4) can be the same as that in the wavelet domain (2).*

Proof: Substituting the wavelet separation (1) into (2), we have

$$\mathcal{C} = \bar{\mathcal{C}} * h_0 * g_0 + \mathcal{F} * h_1 * g_1 \tag{5}$$

Incorporating the perfect reconstruction property of wavelet filters [8], $h_0 * g_0 + h_1 * g_1 = 1$, and $f_l = h_0 * g_0$ into (5) yields

$$\mathcal{C} = \bar{\mathcal{C}} * f_l + \mathcal{F} * (1 - f_l)$$

which is equivalent to (4) due to (3). ■

In addition to having a lower computational complexity, the proposed spatial-domain substitution scheme can address an inherent drawback in the wavelet-domain substitution in [7]. For the latter, since at least half of the values in each color plane are estimated to obtain a full-resolution plane, and the errors of the estimated values mainly reside in high frequencies due to CFA sampling, this limits the accuracy of the reconstructed, reference high-frequency component $\mathcal{F}_{w_h}$, and hence degrades the overall demosaicking quality. To mitigate this limitation, Gunturk *et al.* iterated high-frequency substitution in the wavelet domain several times.

Table 1. PSNR performance (in dB) comparison of substitutions in the wavelet domain and the spatial domain.

Image		Wavelet	Spatial 5-3	Spatial f_s
1	R	33.80	34.87	35.98
	G	34.83	38.08	39.61
	B	33.90	34.99	36.19
2	R	37.30	37.69	37.26
	G	40.92	42.43	41.80
	B	39.83	39.88	39.56
3	R	40.49	41.19	41.20
	G	42.29	44.32	44.11
	B	40.07	40.67	40.63
4	R	36.83	37.32	37.00
	G	40.82	43.36	43.65
	B	40.13	41.02	41.60
5	R	35.35	36.32	36.81
	G	36.02	39.15	39.82
	B	34.87	35.79	36.22

By working in the spatial domain, we can use a simpler and more effective scheme to address the above-mentioned limitation. This is because less amount of interpolation errors will be incurred at the low frequencies $\bar{\mathcal{C}}_{s_l}$, and hence they can be estimated more accurately by low-pass filtering the interpolated plane $\bar{\mathcal{C}}$. Furthermore, since one true color value is available at each pixel (m, n) from CFA samples, subtracting the true color value and the more accurately estimated low frequencies in the corresponding color plane can obtain pixel-accurate high frequencies, as follows:

$$\mathcal{F}_{s_h}(m,n) = \underbrace{\left[\mathcal{C} - \bar{\mathcal{C}}_{s_l}\right]}_{\bar{\mathcal{C}}_{s_h}}(m,n) \tag{6}$$

where $\mathcal{C}(m,n) \triangleq CFA(m,n)$, the accurate color value from CFA samples.

Figure 2 confirms that the proposed method using spatial-domain substitution reduces the artifacts at red and blue CFA samples as compared with that obtained by the wavelet-domain substitution [7]. (Here, we used Hamilton method [2] to obtain the initial full-color planes, and used 5-3 wavelet [9] and its equivalent low-pass filter in the spatial domain, i.e., Eq. (3)). Table 1 shows that the proposed spatial-domain substitution can improve the PSNR performance by up to 3 dB for test Images 1-5 in Figure 3.

To further reduce the computational cost, we can also use a much simpler filter $f_s = [1, 1, 1]^T[1, 1, 1]$ instead of the 5-3 wavelet filter. As shown in Table 1, the filter f_s does not decrease the PSNR performance, but requires only $4MN$ additions and $1MN$ multiplications for the filtering process, far fewer than that of 5-3 wavelet filter.

The proposed spatial-domain high-frequency substitution can be summarized in the following three steps:

1. Interpolate an initial full-color image $\bar{\mathcal{C}}, \mathcal{C} \in \{R, G, B\}$, from CFA data. Apply a low-pass filter $f_l = f_s$ [Eq. (3)] on the initial image to separate its low and high-frequency components, $\bar{\mathcal{C}}_{s_l}$ and $\bar{\mathcal{C}}_{s_h}$.
2. Estimate the reference high-frequency component $\mathcal{F}_{s_h}$ by subtracting the accurate color values from CFA samples and their corresponding low-frequency values using (6).

3. Use $\mathcal{F}_{s_h}$ and (4) to refine the three color planes.

In the substitution experiments reported above, Hamilton method [2] was used for interpolating the initial full-color image. In the next section, we propose an anisotropic interpolation scheme that requires less computational cost and attains a notably better quality.

3. INTERPOLATION OF INITIAL FULL-COLOR IMAGE

We propose here a simple anisotropic interpolation scheme to improve the existing effective color interpolation (ECI) demosaicking method [4]. To exploit both inter-pixel and inter-color correlations, the ECI method interpolates color-difference images as follows:

$$\bar{\mathcal{C}} = \mathcal{I}(\mathcal{C}_s - \mathcal{F}) + \mathcal{F} \tag{7}$$

where $\mathcal{C}_s, \mathcal{C} \in \{R, G, B\}$, is the subsampled plane, $\mathcal{F}$ is the reference full-resolution plane, and $\mathcal{I}$ denotes the interpolation process. The ECI method constructs the green plane and uses it as the reference to interpolate the red and blue planes. Its performance primarily depends on the quality of the constructed green plane. To improve the green-plane interpolation, the ECI method also interpolates the red and blue planes as reference. The method can be summarized by the following steps: 1) Interpolate the red and blue planes at green pixels; 2) Use the red or blue plane as the reference to interpolate the green plane at red or blue samples; 3) Use the green plane as the reference to interpolate the red and blue planes. We improve the ECI method by using an anisotropic interpolation scheme instead of the original isotropic one.

Let $\mathcal{I}_h$ and $\mathcal{I}_v$ be the interpolation results on the horizontal and vertical directions. The ECI's isotropic interpolation averages the results in both directions; that is

$$\mathcal{I} = \frac{\mathcal{I}_h + \mathcal{I}_v}{2} \tag{8}$$

An anisotropic interpolation keeps only the results in the smooth direction. Let w_h and w_v be the edge indicator in the horizontal and vertical directions. A typical anisotropic interpolation [2] works as follows:

$$\mathcal{I} = \begin{cases} \mathcal{I}_h & w_h - w_v \le 0 \\ \mathcal{I}_v & w_h - w_v > 0 \end{cases} \tag{9}$$

However, the anisotropic method may fail in smooth regions, where the image contents in both of the two directions are smooth and an isotropic interpolation (8) could perform better.

To address this problem, we propose using a simple threshold T to combine isotropic (8) and anisotropic (9) interpolations,

$$\mathcal{I} = \begin{cases} \mathcal{I}_h & w_h - w_v < -T \\ \mathcal{I}_h & w_h - w_v > T \\ \frac{\mathcal{I}_h + \mathcal{I}_v}{2} & otherwise \end{cases} \tag{10}$$

This new ternary, anisotropic interpolation scheme identifies a new smooth region–the third class in (10)–and improves the performance in the region. Some existing methods also use similar ternary interpolation, but with $T = 0$ [2], which sometimes misclassifies smooth regions as edge regions.

To show the improvement, we apply the interpolation schemes (9) and (10) in Step 2 of the ECI method [4] because the green plane is essential for interpolating the red and blue planes. This operation also requires less computational cost as there are fewer missing green values. We use a simple edge indicator as described in [2] to compute the weights w_h and w_v, and set $T = 20$ based on a small set of test images.

Table 2. PSNR performance (in dB) comparison of anisotropic interpolations.

Image		Hamilton	ECI	ACI	TACI
1	R	33.25	32.66	33.52	34.07
	G	34.83	35.33	34.81	35.54
	B	33.36	32.80	33.61	34.17
2	R	36.95	34.39	37.22	37.45
	G	40.92	39.16	40.91	41.69
	B	39.43	36.69	39.56	40.04
3	R	39.97	37.21	40.35	40.98
	G	42.29	40.91	42.29	43.24
	B	39.85	37.71	39.70	40.21
4	R	36.34	36.40	36.35	36.64
	G	40.82	41.37	40.96	41.95
	B	39.45	38.89	40.12	41.02
5	R	34.74	33.92	34.87	35.36
	G	36.02	36.29	36.00	36.60
	B	34.43	33.97	34.40	34.85

Table 2 shows that the proposed ternary anisotropic color interpolation (TACI) yields the best PSNR results. TACI improves the performance about 2 dB on average compared to isotropic-based ECI, and 0.6 dB compared to anisotropic color interpolation (ACI). Note that the two anisotropic interpolations have nearly the same computational complexity. As for Hamilton demosaicking [2], its PSNR performance is 0.8 dB worse than TACI, and it also requires about two times the computational cost. Specifically, Hamilton demosaicking requires $21MN$ additions, $11MN$ shifts, $8MN$ absolutes, and $1MN$ comparisons, while the proposed TACI needs only $12MN$ additions, $4MN$ shifts, $2MN$ absolutes, and $1MN$ comparisons.

4. PERFORMANCE COMPARISON

In this section we compare the performance of the proposed spatial-domain high-frequency substitution (SHFS) with several recent state-of-the-art demosaicking methods: Alternating Projections (AP) [7], Successive Approximation (SA) [6], Frequency Selection (FS) [5], and Frequency Domain Method (FDM) [3].

4.1. Demosaicking results

Table 3 shows the PSNR performance of the proposed and the comparison methods. On average, the improvement of the proposed method is around 0.5 dB to AP, 0.7 dB to SA, and 1.7 dB to FS. As for FDM, which also uses an anisotropic interpolation scheme, its performance is comparable to our proposed method at the cost of much higher complexity (see Section 4.2).

Figure 4 compares the perceptual results of these methods, and shows that our proposed method obtains the best perceptual results with sharper edges and fewer zipper artifacts. Severe zipper artifacts are produced around the edges obtained by the AP, SA, and FS methods due to the use of isotropic techniques. The FDM method can obtain better results but some artifacts remain because its energy criteria for estimating the edge direction may not be as accurate in some image regions.

4.2. Complexity

Table 4 summarizes the computational complexity of the proposed method and the comparison methods. For simplicity, we consider

Table 3. PSNR performance (in dB) comparison.

Image		AP	SA	FS	FDM	SHFS
1	R	36.59	36.66	35.06	37.03	36.41
	G	40.49	40.88	39.64	41.05	40.31
	B	36.86	37.64	35.45	37.20	36.63
2	R	35.87	35.54	34.04	37.08	37.29
	G	40.81	40.06	39.70	41.87	42.09
	B	38.60	39.07	36.57	38.74	39.71
3	R	40.43	39.08	38.67	41.25	41.39
	G	43.48	42.21	42.20	44.12	44.28
	B	40.39	39.36	38.49	40.45	40.84
4	R	36.68	36.17	35.19	37.11	37.02
	G	43.33	42.64	42.99	44.68	43.97
	B	41.43	40.88	40.76	42.49	42.15
5	R	36.82	35.59	34.96	37.38	37.04
	G	39.81	38.27	38.46	40.57	40.17
	B	36.55	35.34	34.80	36.69	36.47
6	R	37.72	37.22	36.24	39.86	37.99
	G	41.52	41.40	40.81	43.12	41.44
	B	37.27	36.67	35.66	38.23	37.11
7	R	40.84	40.12	38.89	41.50	41.56
	G	43.62	42.67	42.44	44.83	44.10
	B	39.92	39.35	38.08	40.43	40.56
8	R	34.06	34.44	31.42	34.29	34.36
	G	38.59	38.74	36.60	38.66	38.50
	B	34.29	35.00	31.57	34.28	34.37
9	R	40.54	40.60	38.68	40.97	41.20
	G	43.26	43.33	42.34	44.00	44.61
	B	41.43	41.36	39.73	42.34	42.71
10	R	40.55	40.12	39.28	40.94	40.90
	G	43.89	43.86	43.55	44.70	45.00
	B	40.68	40.56	40.07	41.41	41.48
Average	R	36.95	36.66	35.63	37.57	37.30
	G	40.49	40.24	39.80	41.26	40.94
	B	37.31	37.10	35.89	37.59	37.51

Table 4. Comparison of demosaicking complexity.

Method	No. of computational operations	
	Additions	Multiplications
AP	$384MN$	$384MN$
SA	$37.5\text{-}53.5MN$	$12.75\text{-}21.25MN$
FS	$124MN$	$21MN$
FDM[1]	$40\log_2(MN)MN$	$20\log_2(MN)MN$
Ours	$34MN$	$3MN$

the cost of a shift, absolute, or comparison operation the same as that of an addition operation since they all can be completed in one clock cycle. The computational costs of the comparison methods are either taken directly from the original papers (AP [7] and SA [6]), or obtained based on our analysis of the algorithms described in the respective papers (FS [5] and FDM [3]). It follows from Table 4 that our method requires the fewest numbers of multiplications and additions. In particular, the FDM method, which yields comparable PSNR performance, requires over 100 times of multiplications and 20 times of additions when compared with the proposed method.

5. CONCLUSIONS

We have proposed in this paper an efficient and effective CFA demosaicking method. Our proposed method substitutes the high-frequency information between color planes in the spatial domain instead of in the wavelet domain. The spatial-domain substitution not only can reduce the computational cost greatly, but also improve the high-frequency estimation and the substitution performance. A ternary anisotropic interpolation scheme is also proposed to obtain the initial full-color planes required for the substitution. Compared to four recent state-of-the-art methods, the experimental results show that our proposed method yields better PSNR performance and perceptual results and requires the least computational cost.

[1]The complexity analysis is based on performing convolution using FFT for its simplicity. For example, considering the size of test images used in our experiments ($M = 512$ and $N = 768$), the numbers of additions and multiplications required are $743MN$ and $372MN$, respectively. Performing direct spatial filtering requires $1833MN$ additions and $1833MN$ multiplications.

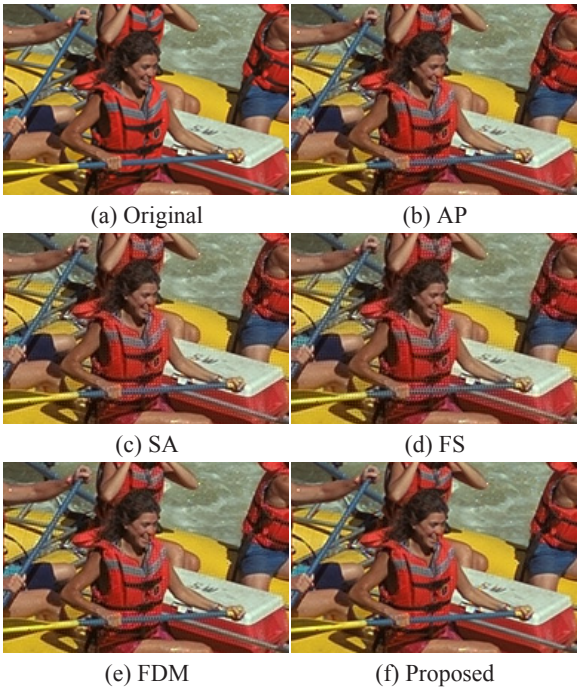

(a) Original (b) AP (c) SA (d) FS (e) FDM (f) Proposed

Fig. 4. Original and demosaicked results of a cropped region

6. REFERENCES

[1] B. Bayer, "Color imaging array," *United States Patent*, no. 3,971,065, 1976.

[2] J. Hamilton and J. Adams, "Adaptive color plane interpolation in single sensor color electronic camera," *United States Patent*, no. 5,629,734, 1997.

[3] E. Dubois, "Frequency-domain methods for demosaicking of bayer-sampled color images," *IEEE Trans. Signal Processing Letters*, vol. 12, no. 12, pp. 847–850, Dec. 2005.

[4] S. C. Pei and I. K. Tam, "Effective color interpolation in CCD color filter array using signal correlation," *IEEE Trans. on cirduits ans systems for video technology*, vol. 13, no. 6, 2003.

[5] D. Alleysson, S. Susstrunk, and J. Herault, "Linear demosaicking inspired by human visual system," *IEEE Trans. on Image Processing*, vol. 14, no. 4, pp. 439–449, 2005.

[6] X. Li, "Demosaicing by successive approximation," *IEEE Transcations on Image Processing*, vol. 14, no. 3, pp. 370–379, 2005.

[7] B. K. Gunturk, Y. Altunbasak, and R. M. Mersereau, "Color plane interpolation using alternating projections," *IEEE Trans. on Image Processing*, vol. 11, no. 9, 2002.

[8] I. Daubechies, "Orthonormal bases of compactly supported wavelets," *Communications on Pure and Applied Mathematics*, vol. 16, pp. 909–996, Jan. 1988.

[9] M. Vetterli and C. Herley, "Wavelets and filter banks: theory and design," *IEEE Trans. on Signal Processing*, vol. 40, pp. 2207–2232, Sept. 1992.